Comparison of Anthropomorphic Test Dummies with a Pediatric Cadaver Restrained by a Three-point Belt in Frontal Sled Tests

J. H. Ash[1], C. P. Sherwood[1], Y. Abdelilah[1], J. R. Crandall[1], D. P. Parent[1] and D. Kallieris[2]
[1] University of Virginia Center for Applied Biomechanics; [2] University of Heidelberg

ABSTRACT

Validation data for assessing dummy child biofidelity are limited, especially with regard to whole-body kinematics. Therefore, the goal of this study was to assess the kinematic biofidelity of current child dummies relative to results obtained from the analysis of a child cadaver sled test. The baseline data were obtained from a previously unpublished test performed with a 13 year-old pediatric cadaver restrained by a three-point belt. The cadaver test conditions were reconstructed using two dummies with anthropometry closest to that of the cadaver, the HIII 10-year old and HIII 5th female (~size of 12-year old) dummies. In addition to photo targets, the cadaver was instrumented with head accelerometers. The test dummies were equipped with triaxial accelerometers in the head, chest, and pelvis; load cells in the upper neck, lower neck, and lumbar region; and a chest deflection sensor. Due to anthropometric differences between the dummies and the child cadaver, geometric scaling was performed based on the seated height and material properties. To validate the scaling, comparisons among dummy sizes were performed as a first step before comparing to the child cadaver data. Kinematic evaluations of head, hip, and knee trajectories were obtained from film analysis. Accelerations of the head, shoulder and lap belt loads were measured and compared among the scaled dummy and child cadaver data. While this study shows that the HIII 10-year old and HIII 5th female reasonably approximate the shoulder belt force, the resultant head acceleration, and the maximum head excursion of a 13-year old pediatric cadaver, differences in dummy kinematics were identified that resulted in deviations in the trajectories and the peak head acceleration following head strike to the chest. Some of these deviations in dummy kinematics were attributed to nonbiofidelic motion of the rigid thoracic spine. Specifically, the dummies exhibited extensive bending at the junction of the cervical and thoracic spine that resulted in modified head kinematics. In addition to new cadaver data, the paper provides insight into the applicability of geometric scaling for dummy evaluation and suggestions for improved dummy biofidelity.

INTRODUCTION

The design of current child restraint systems relies heavily on the biofidelity of current anthropometric test devices. Given the paucity of biomechanical data available for both development and validation of child dummies, child response targets have largely been achieved through geometric and material property scaling of adult responses. This scaling, however, involves a number of assumptions in terms of geometric similarity that may not be justified with the differences in regional dimensions and mass distributions between children and adults (e.g., the child head comprises a disproportionate share of the overall body mass relative to the adult head). Furthermore, the scaling of response for material property from adults to children are usually limited to one tissue type (e.g., bone) whereas the actual response of a body region may involve the composite response effects of a large number of soft and hard tissue types. Therefore, it is essential that dummies are evaluated under whole body loading conditions similar to the test environment in which they will be used to design restraint systems. While reconstructions of crashes involving children provides valuable injury data, the lack of information regarding initial occupant, restraint, and vehicle conditions introduces large uncertainties into reproducing these events in the laboratory for the purpose of dummy validation. For the validation of occupant kinematics, pediatric cadaver tests arguably provide the best condition for evaluation of dummy seat belt and booster seat restraint of children (Kallieris, 1976). In the study presented here, data from a sled test using a 13-year old cadaver was analyzed and compared to a series of tests conducted with dummies under identical test conditions to those of the pediatric cadaver. The two anthropomorphic test devices (ATD) that were closest in size to the pediatric cadaver were used including the Hybrid III (HIII) 10-year old and Hybrid III 5% adult female (AF5) (~size of 12 year old). The tests and analysis in this paper compare the pediatric cadaver kinematic and kinetic data to the data obtained using the dummies.

METHODS

Pediatric cadaver

The pediatric test used for the sled tests involved a 13-year old cadaver positioned in a mid-1970's Volkswagen Golf Type 1 seat and restrained by a high elongation (17%) three-point belt. The impact velocity of the sled was 41 km/h and the pulse was trapezoidal with a median sled deceleration of 21 g. Black and white photos were taken before and after the test and high speed cameras acquired lateral and frontal views with frame rates of 1000 frames/s and 500 frames/s, respectively. Photo targets were placed on the head, shoulder, and pelvis of the cadaver (Figure 1a) and were later used in video analysis using a commercial software package (Phantom Camera Control, Version 8.1.607 XP). The cadavers were instrumented with X and Z axis accelerometers fixed to the side of the head at the lateral projection of the head center of gravity (CG). In order to conform with the SAE J211 standard coordinate system (SAE, 2003), the Z axis component from the original data collection (Figure 1b) was inverted to ensure it was positive in a downward direction. In addition to the head and buck accelerations, forces were measured in the shoulder and lap belts.

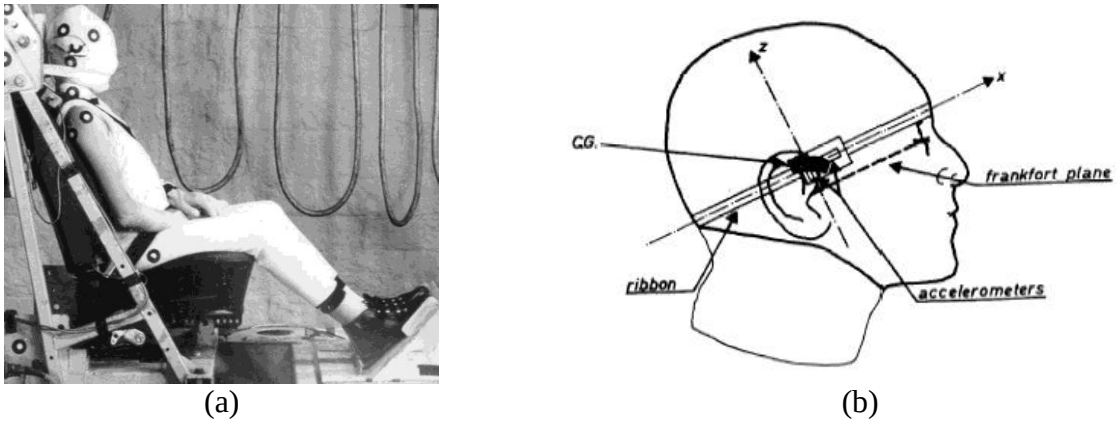

(a) (b)

Figure 1: a) Seated position of the pediatric cadaver and placement of photo targets. b) Mounting diagram of accelerometers in the pediatric cadaver test (from Kallieris, 1976).

The pediatric cadaver data was taken from an unpublished test performed at the University of Heidelberg in 1976. Though the test analyzed in this study comes from an unpublished test, information about the general test setup can be found in Kallieris (1976). The Kallieris (1976) study uses pediatric cadavers and child restraint systems, which differs from the pediatric cadaver used in this study but further information is contained in that study that further investigators may find useful.

Anthropometric test dummies

Subsequent to the pediatric cadaver test, tests with anthropometric dummies were designed to duplicate the experimental conditions of the cadaver using the UVA sled system (Via Systems Model 713). The test fixture, or "buck," consisted of the front passenger bucket seat of a 1975 Volkswagen Golf with matched anchorage locations for the seatbelts. The seat-adjustment mechanism was removed to make it more durable for repeated testing, and both the seat pan and seat back were rigidly fixed to the buck. The three-point belt was a custom-made, approximate replica of the original belt with 18% elongation webbing.

The tests designed to duplicate the test conditions of the pediatric cadaver were three HIII 10-year old tests and two AF5 tests. The dummies were calibrated prior to the testing, and all joints were adjusted to the relevant specification (1 g). The dummy was instrumented with accelerometers and angular rate sensors in the head (CG), accelerometers in the chest (CG) and pelvis, load cells in the upper and lower neck, femur, left and right ASIS, and clavicle. In addition, the dummies were modified to allow for attachment of instrumentation cubes containing accelerometers and angular rate sensors on the upper thoracic spine. Though the X, Y and Z components of the head CG acceleration were measured, only the X and Z were used in the calculation of the resultant acceleration as was done in the collected pediatric cadaver data.

Before placing the dummy in the seat, photo targets were attached to the dummy at the head CG, hip, knee, ankle, shoulder, and points along the thigh. Other photo targets were placed at measured distances on the test fixture in order to provide spatial resolution in various planes for the video analysis. The dummy was positioned in the Volkswagen seat according to the procedure developed by Reed (2006). This procedure made modifications on the specifications

of FMVSS 213 in order to more accurately model real world child seated posture. After the dummy was centered, a force of 178 N was first applied to the pelvis and then to the thorax of the dummy to ensure it was properly seated. At this point, minor adjustments were made to ensure the dummy's position matched that of the cadaveric test by using the photos taken before the cadaveric test was performed. With the dummy firmly positioned in the seat, the three point belt was positioned and buckled. Belt tension load cells (Interface Model DK113523) were attached to the outboard lap and shoulder portions of the belt.

The tests were recorded using three high-speed (1000 frames/s) digital video imagers (Kodak RO) that were positioned to provide a perpendicular view from the driver's side of the sled track, an oblique view from the front/passenger side, and an overhead view. Photo target trajectories were tracked using video analysis software (Phantom Camera Control, Version 8.1.607 XP). To ensure test to test repeatability, a three dimensional positioning device (Faro arm) was used to confirm the initial condition of each dummy prior to launching the sled. In addition, photos were taken to record the pre-crash and post-crash position and orientation of the dummies.

Geometric scaling

In order to compare the kinematics, the accelerations and loads of the dummies and the pediatric cadaver were scaled. The scaling methods take into account variations in subject anthropometry in order to calculate equivalent values between the two subjects and are based on dimensional analysis (Irwin, 1997 and Irwin, 2002). The nondimensional ratio used in the scaling analysis is the length scaling ratio,

$$\lambda_L = \frac{L_1}{L_2} \qquad [1]$$

where λ_L is the scaling factor, L_1 is the seated height of the reference subject, the subject to be scaled to, and L_2 is the seated height of subject to be scaled. The seated height was used in the length scaling factor since this information was known for both the cadaver and the dummies. In addition to the length scaling factor the other fundamental nondimensional ratio used was the modulus of elasticity ratio λ_E. In order to scale the forces, accelerations and event times the following scale factors were used,

$$\lambda_A = \frac{1}{\lambda_L}, \qquad [2]$$

$$\lambda_F = \lambda_K \lambda_L, \qquad [3]$$

$$\lambda_T = \frac{\lambda_L}{\lambda_E^{0.5}}, \qquad [4]$$

where λ_A is the acceleration scaling factor, λ_F is the force scaling factor and λ_T is the time scaling factor from Irwin (1997). The force scaling factor was based on the ratio of the stiffness of the subjects' chests, λ_K. This chest stiffness ratio takes into account the difference in stiffness of the subjects' ribs along with the contribution that the viscera and flesh have on the overall stiffness of the chest. The development of the chest stiffness ratio can be found in Appendix A.

The heights, elastic moduli, and masses used in this scaling approach along with the scale factors can be found in Table 1. The value of the Elastic Modulus for the HIII 10-year old was found in Irwin (2002) and the value of the elastic modulus for the 13-year old pediatric cadaver was estimated from interpolating between data points provided by Irwin (1997).

Once the values of the accelerations and forces were scaled the maximums, and minimum in the case of the head CG X component, were found and compared. Since three repeat tests were performed with the Hybrid III 10-year old dummy, the average and standard deviations of responses could be calculated. For the pediatric cadaver and Hybrid III 5th female dummy, there were an insufficient number of tests to calculate standard deviations. Since direct comparison of point estimates (i.e., average response values at any time t) would not have accounted for test variability inherent in even laboratory dummy tests, a methodology of generating estimates of confidence intervals was created. In order to compare dummy and cadaver responses, a normal distribution was assumed around the mean response. The upper and lower bounds of the 95% confidence interval were estimated using,

$$UB = (1 + COV * z)\mu$$
$$LB = (1 - COV * z)\mu \qquad [5]$$

where UB and LB are the upper bound and lower bound, respectively, COV is the coefficient of variance, z is the number of standard deviations to achieve the desired confidence interval, and μ is the mean of the quantity the boundaries are found for. The COV that was used for the dummies was 10% because this was stated as the upper limit of acceptable values in the automotive safety field by Shaw (1994).

Table 1: Scale factors (compared to HIII 10-year old) and surrogate measurements

	HIII 10yo	HIII AF5	Pediatric Cadaver
Seat Height, [m]	0.72	0.79	0.81
Elastic Modulus, [GPa]	8.45	9.9	9.0
Mass, [kg]	35.0	49.1	50.0
λ_L	1	0.91	0.89
λ_E	1	0.85	0.94
λ_A	1	1.10	1.13
λ_K	1	0.85	0.89
λ_F	1	0.77	0.79
λ_T	1	0.99	0.92

The length scaling factor was applied to the kinematic trajectories obtained from the video analysis. The lap and shoulder belt loads as well as the head center of gravity accelerations were scaled by the force and acceleration scaling factors, respectively. In order to scale the whole body kinematics of the various test subjects, a common reference origin was created to account for differences in local origins among the dummies of different sizes (Figure 2). The common point that was chosen for comparing these tests was the point directly below the H-point in the vertical direction to where the subject meets the seat.

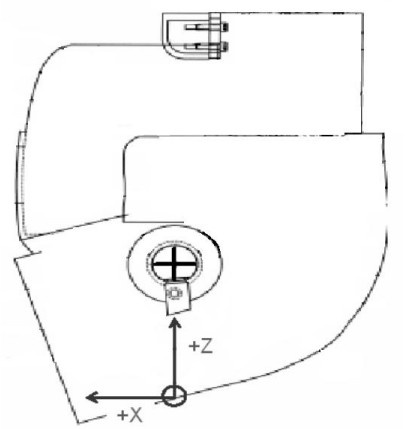

Figure 2: Location of common reference origin where the black cross represents the H-point of the dummy and the origin of the reference coordinate system is shown directly below H-point. (Adapted from NHTSA 2000)

For the dummies the H-point information was found from the technical specification drawings and the reference manuals for each dummy (HIII 10-year old: NHTSA 2005, AF5: NHTSA 2000). In order to determine an appropriate value of the vertical distance from the H-point in the pediatric cadaver, scaling was used. Since no measured value for this distance was included in the anthropometry, the known value of the vertical distance was taken for the HIII 6-year old and scaled, using the length scaling factor, to the approximate distance for the cadaver.

Video Analysis

To assess the kinematics of each surrogate, the points of interest from the videos were the head CG, the shoulder, the H-point, and the knee joint. Subsequently, the pixel trajectory values were converted to a quantitative measurement using the spatial resolution of the imager in the plane of the surrogate. Once the conversion into spatial dimensions was completed, the trajectories of the points of interest were filtered using the convention specified in ISO/DIS 13232-4 (ISO, 2004). This filter is a four pass moving average filter designed to smooth the data.

The points of interest were easily tracked from the tests involving the dummies since the photo targets had been placed on the dummy at the specific locations and then tracked using the software package. It was considerably more difficult to determine the location of these points in the cadaver test because the desired location was either not available for direct measurement (i.e., a photo target had not been placed at that location) or the photo targets were placed on clothing that moved during the impact event. Therefore, several hybrid techniques were developed to account for either the lack of targets at a location or local movement of a target. These techniques are discussed in detail in Appendix B of this paper.

RESULTS

Scaling accelerations and forces

Before the method of scaling (Equations 2, 3, and 4) was used to qualify the performance of the dummies relative to the cadavers, the applicability of scaling techniques for the sled environment was verified. In other words, we determined the extent of the violations of the assumptions related to geometric similarity (i.e., the assumption that the dummies responses are scaled versions of each other) and homologous loading points (i.e., the assumption that if the belt loads a particular point in one sized dummy it loads the same point in another) by assessing the effectiveness of scaling the dummy responses to each other. Since the dummies were developed with the same dimensional analysis scaling procedures utilized in our analysis, we reasoned that a dummy's response should be scalable to that of another dummy if the assumptions of geometric similarity and homologous loading are not drastically violated. In order to test this assumption, the responses of the HIII 10-year old were compared to the scaled responses of the Hybrid III 5th female. It was seen that the acceleration and seat belt forces were able to be scaled and produce comparable results (this is examined in Appendix C).

After determining that the scaling method was able to yield comparable results between the two dummies, it was then used to scale the seat belt load and head CG acceleration (Figure 3 a & b).

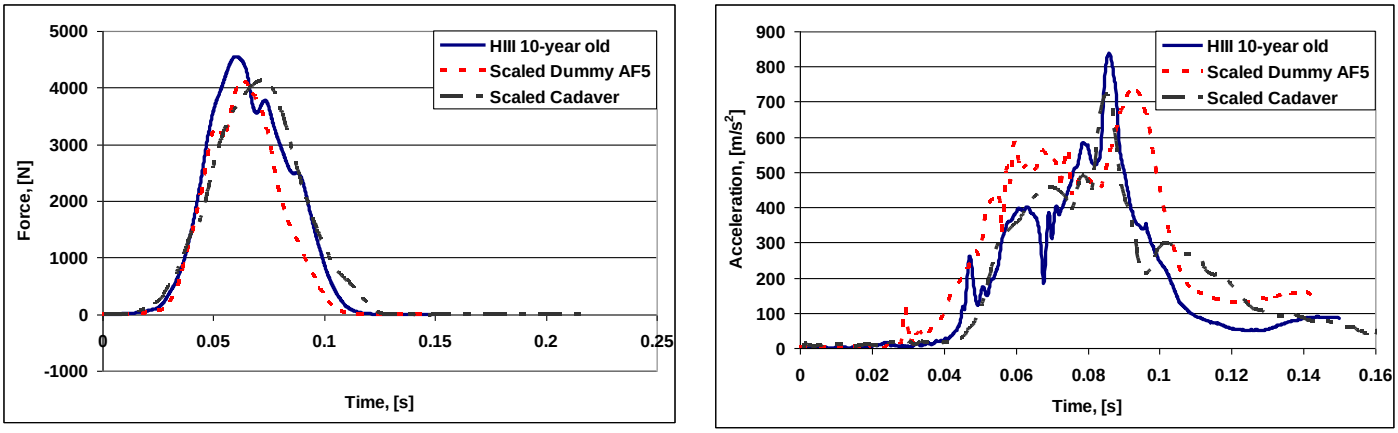

(a) (b)

Figure 3: Scaled values of the AF5 and pediatric cadaver graphed with the values of the HIII 10-year old for the shoulder belt (a) and resultant head CG acceleration (b).

The additional graphs of the scaled lap belt load and X and Z components of the head CG acceleration are included in Appendix D. In Figure 3 a & b it is seen that the general trend of the data along with the peak value are similar between the scaled values of the AF5, scaled pediatric cadaver, and the HIII 10-year old.

The upper and lower bounds found in
Table 2 were found using Equation 5 using the average values and 95% confidence intervals, z = 1.96. In order to use Equation 5 to find the upper and lower bounds for the scaled AF5 a coefficient of variance must be assumed since the sample size is insufficient (n = 2) to determine a standard deviation. As was stated earlier the COV from Shaw (1994) of 10% will be assumed in order to determine the upper and lower bounds.

Table 2: HIII 10-year old, Scaled AF5, and Scaled pediatric cadaver values

		HIII 10-year old					Scaled AF5			Scaled Pediatric Cadaver
		Average	St. Dev.	COV	Upper bound	Lower bound	Average	Upper bound	Lower bound	Value
Belt Forces, [N]	Lap	3999	325	0.081	4782	3215	4119	4926	3312	2886
	Shoulder	4545	64	0.014	5436	3654	3976	4756	3197	4119
Head CG, [m/s^2]	X	-1085	267	-0.246	-1298	-872	-715	-855	-575	-352
	Z	551	81	0.147	659	443	542	649	436	663
	Resultant	1086	266	0.245	1299	873	739	884	594	720
Pre-strike Head CG, [m/s^2]	X	-189	3	-0.018	-226	-152	-235	-281	-189	-352
	Z	404	29	0.070	484	325	542	649	436	296
	Resultant	427	39	0.092	511	343	569	681	457	456
Chest CG, [m/s^2]	X	-459	12	-0.026	-549	-369	-553	-661	-445	
	Y	71	41	0.574	85	57	53	64	43	
	Z	-401	134	-0.333	-480	-323	-127	-152	-102	
	Resultant	501	72	0.144	599	403	573	685	461	

Kinematic scaling

In order to first validate the technique of length scaling for kinematic factors, the trajectories of the HIII 10-year old and the Hybrid III 5th were compared. It was found that scaling between the dummies was able to provide good agreement of the kinematic trajectories and the method is validated. This is examined in greater detail in Appendix B under the Kinematic scaling section. Scaling the pediatric cadaver trajectories to the HIII 10 and AF5 dummy sizes (Figure 4 a & b) resulted in similar maximum head excursion values (Table 3) and H point trajectories.

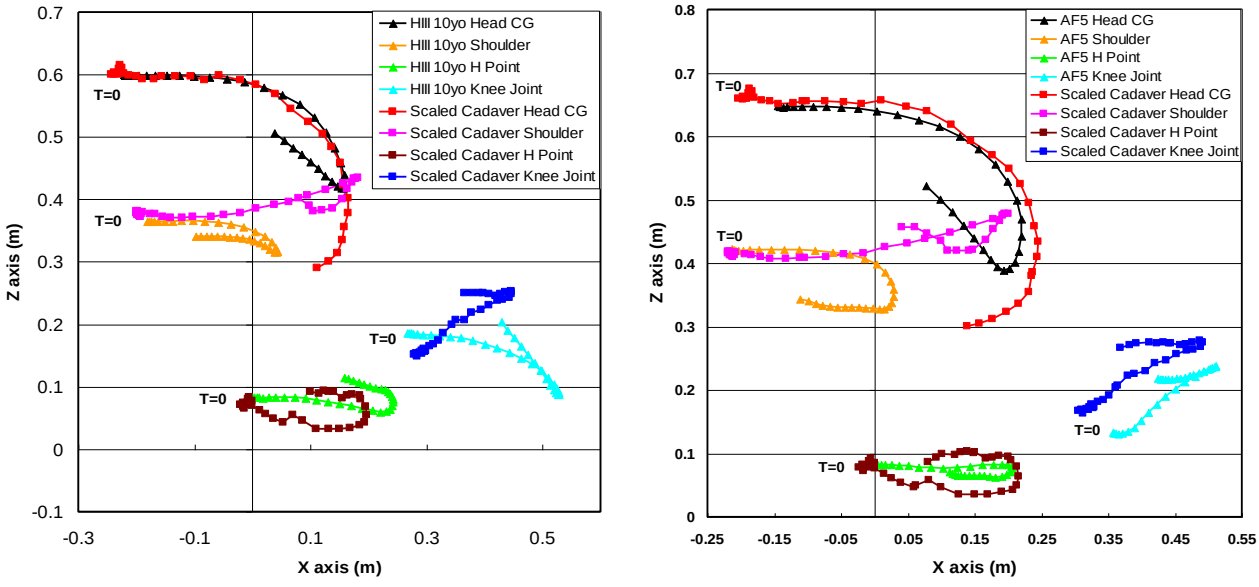

(a) (b)

Figure 4: a) HIII 10-year old and scaled pediatric cadaver kinematic trajectories. b) AF5 and scaled pediatric cadaver kinematic trajectories.

The head excursion values in Table 3 are the maximum X distance that the head CG traveled past the origin in the +X direction. The percent difference calculation is based on this excursion of the pediatric cadaver. The differences in the knee joint trajectories with the cadavers (Figure 4a) resulted from the HIII 10-year old foot not contacting the floor of the buck. The differences in the shoulder trajectories in Figure 4 a&b were due to the rigid spine and shoulder assembly that are part of the HIII dummies. As the cadaver engaged the seat belt, the shoulder and upper body bent over the shoulder belt, causing a larger travel distance of the shoulder.

Table 3: Percent Difference between dummies and pediatric cadaver in head excursion

	Cadaver Scaled to:	
	HIII 10-year old	AF5
Cadaver, [cm]	16.5	24.6
Dummy, [cm]	15.8	22
% Difference	4.4%	11.8%

Differences in kinematics

Though the head excursions of the dummies and the scaled cadaver produced results that were similar, the mechanism in which these excursions were achieved is quite different. In order to determine the way in which the dummies and the pediatric cadaver reach their points of maximum excursion, points were digitized along the approximate location of the spine and head using the video analysis software. These points along the spine to the base of the skull, then to the most posterior point of the skull or and ending with the most superior point of the skull will be referred to as the spinal contour. The spinal contours are taken in 10 ms intervals back from the time of maximum excursion, labeled t = 0 ms, for 70 ms and include one contour after the time of maximum excursion for both the pediatric cadaver (Figure 5 a) and HIII dummy (Figure 5 b).

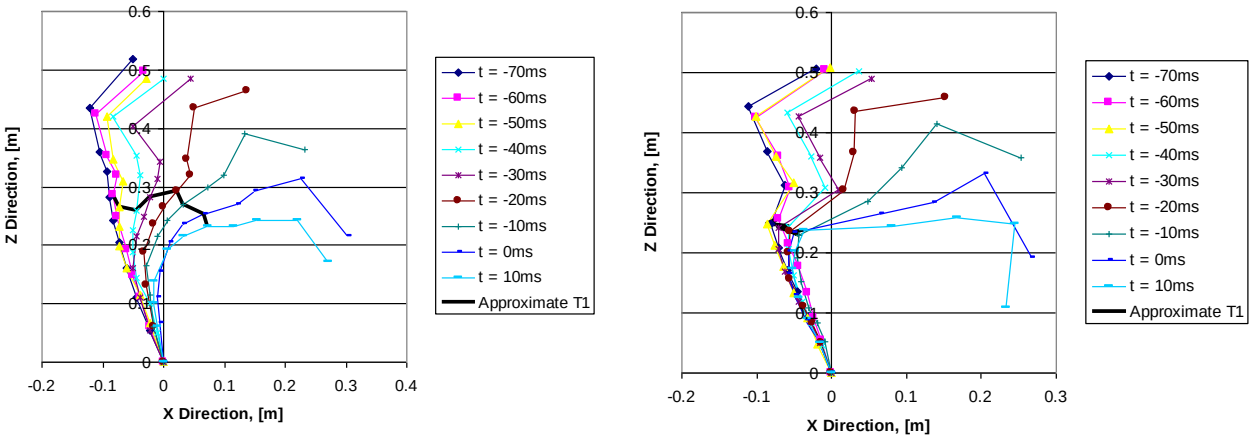

(a) (b)

Figure 5: Spinal contours of the pediatric cadaver (a) and HIII dummy (b) with approximate T1 location shown during motion

The approximate location of the T1 vertebra was tracked along with other points along the spine and head to form the spinal contour for the HIII dummy (Figure 5 a & b). It was observed that the T1 vertebra travels more in the pediatric cadaver, which is certainly expected given the rigid nature of the HIII spine. In order to compare the relative horizontal displacement of T1 between the surrogates the displacement relative to the initial position of the approximate location of T1 was found when the most distal point of the spine is held fixed. The T1 displacement of the cadaver is much larger than that of the HIII dummy, as seen in Figure 5 a & b, caused by noticeable bending of the thoracic region of the pediatric cadaver's spine. This result is consistent with observations made by Sherwood (2002), where it was found that the non-biofidelic thoracic spine of the HIII 6-year old produced unrealistically high flexion moments in the dummy's lower neck. Additionally shown by Sherwood (2002) in crash simulations was that additional thoracic spine flexibility decreases all forces and moments in the neck and improves the dummy's kinematics relative to the cadaver's.

LIMITATIONS

A limitation of this study is that there is only one pediatric cadaver was used in the analysis. The approximations used in determining the head CG location, knee joint and H point location all provide reasonable estimations, but are still approximate methods for determining the desired location.

CONCLUSION

This study found that scaling techniques provided reasonable results when scaling between the dummies. When comparing between the dummy and the pediatric cadaver, the scaling techniques reasonably predicted the shoulder belt force, head CG resultant acceleration and occupant head kinematics. Though the scaling techniques for the occupant kinematics were able to produce comparable results between the cadaver and the HIII 10-year old and AF5, this does not necessarily indicate that the cadaver could be scaled to the any size child dummy. Violations in geometric similarity (i.e. different loading locations of the belt on the dummies of different size and seating position between subjects) would likely have a large influence on the scaling results. This study also showed that the rigid spine of the dummy greatly inhibits its biofidelity in head CG and torso kinematics. As shown in the Sherwood (2002) and this study in the lack of non-biofidelic head movement, increasing the flexibility of the spine of the dummies would produce more accurate dummy head CG kinematics. With the information gained in this study, important data into the kinematics and kinetics of children are gained, that, in turn, can be used in the further development of child dummies. Areas where the dummy responses are shown to be non-biofidelic, the rigid thoracic spine for example, can be improved with the data collected in this study being a possible target for the improved response.

ACKNOWLEDGMENTS

We would like to thank NHTSA for their support of the dummy tests although the opinions expressed in this paper are solely those of the authors. The authors would also like to thank TRW for providing the high elongation webbing for the dummy tests.

REFERENCES

IRWIN, A. L. AND MERTZ, H. J., (1997) Biomechanical basis for the CRABI and Hybrid III child dummies. Paper SAE 973317. Proc. 41st Stapp Car Crash Conference, pp. 1-12. Society of Automotive Engineers, Warrendale, PA.

IRWIN, A. L., MERTZ, H. J., ELHAGEDIAB, A. M., MOSS, S. (2002) Guidelines for assessing the biofidelity of side impact dummies of various sizes and ages. Paper SAE 2002-22-0016. Stapp Car Crash Journal, Vol. 46, Nov. 2002, pp. 297-319. Society of Automotive Engineers, Warendale, PA.

ISO TC 22/SC 22/WG 22. Motorcycles—test and analysis procedures for research evaluation of rider crash protective devices fitted to motorcycles—Part 4: Variables to be measured, instrumentation and measurement procedures. ISO/DIS 13232-4, August 31, 2004, Copyright ISO, 2004.

KALLIERIS, D., BARZ, J., SCHMIDT, G., HEESS, G., MATTERN, R. (1976). Comparison between child cadaver and child dummy by using child restraint systems in simulated collisions. Paper SAE 760815. Proc. 20th Stapp Car Crash Conference, pp 511-542. Society of Automotive Engineers, Warrendale, PA.

KENT, R., MURAKAMI, D., KOBAYASHI, S. (2005) Frontal thoracic response to dynamic loading: The role of superficial tissues, viscera, and the rib cage. 2005 International Conference on the Biomechanics of Impacts (IRCOBI) Prague, Czech Republic.

KU, H.H., (1969) Statistical concepts in metrology. In Precision Measurements and Calibration: Statistical Concepts and Procedures, Special Publication 300, Vol. 1. pp. 296-330. Edited by Ku, H.H., United States Department of Commerce, National Bureau of Standards, Washington, D.C.

NATIONAL HIGHWAY TRAFFIC SAFETY ADMINISTRATION (NHTSA). (2000) U.S. DOT/NHTSA - Report - Hybrid III 5th Percentile Small Adult Female Crash Test Dummy - Drawings. Document NHTSA-2000-6940-16.

NATIONAL HIGHWAY TRAFFIC SAFETY ADMINISTRATION (NHTSA). (2005) US DOT/NHTSA - HIII-10C drawing package. Document NHTSA-2005-21247-4.

REED, M. P., SCHNEIDER, L. W., KLINICH, K. D., MANARY, M. A., EBERT-HAMILTON, S. M. Improved positioning procedures for 6YO and 10YO ATDs based on child occupant postures. Paper SAE 2006-22-0014. Stapp Car Crash Journal, Vol 50, Nov. 2006, pp. 337-388. Society of Automotive Engineers, Warrendale, PA.

SAE (2003) SAE J211/1 Instrumentation for Impact Test. Part 1. Electronic Instrumentation. Society of Automotive Engineers, Warrendale, PA, 2003.

SHAW, G., ROY, P., SCHNEIDER, L. W., SCAVNICKY, M., LAPIDOT, A. (1994) Interlaboratory study of proposed compliance test protocol for wheelchair tiedown and

occupant restraint systems. Paper SAE 942229. Proc. 38th Stapp Car Crash Conference, Nov. 1994, pp. 355-370. Society of Automotive Engineers, Warendale, PA.

SHERWOOD, C. P., KALLIERIS, D., EICHELBERGER, M. R., ORZECHOWSKI, K. M., CRADALL, J. R., GUPTA, P. K., KENT, R. W., VAN ROOJ, L., SHAW, C. G. (2002) Prediction of cervical spine injury risk for the 6-year-old child in frontal crashes. Proc. Association for the Advancement of Automotive Medicine, 46th annual conference. Association for the Advancement of Automotive Medicine, 2002, pp. 231-247.

SNYDER, R. G., SCHNEIDER, L. W., OWINGS, C. L., REYNOLDS, H. M., GOLOMB, D. H., SCKORK, M. A., (1977) Anthropometry of infants, children and youths to age 18 for product safety design. UM-HSIR-77-17, Consumer Product Safety Commission http://ovrt.nist.gov/projects/anthrokids/

APPENDIX A: Stiffness Scaling Development

This Appendix provides a discussion and shows the development of the chest stiffness scaling that is used in scaling the shoulder and lap belt forces. Since scaling the forces by the modulus scaling factor alone would seem to neglect the effect of the flesh and the viscera on the magnitude of the scaled belt forces, an alternative way was developed.

Dimensional analysis scaling techniques state that forces are scaled by modulus and length as,

$$\lambda_F = \lambda_E \lambda_L^{\,2} \qquad \text{[A1]}$$

and since it is also known that stiffness would scale by modulus and length as,

$$\lambda_K = \lambda_E \lambda_L \qquad \text{[A2]}$$

it is shown that force can also be scaled as,

$$\lambda_F = (\lambda_E \lambda_L)\lambda_L = \lambda_K \lambda_L \qquad \text{[A3]}$$

The reason that the chest stiffness cannot be scaled simply by the modulus and length, as was shown above, is that there are differences in the child and adult thorax. These differences are not accounted by scaling only by the elastic modulus of the ribs and therefore another approach was taken. Using normalized stiffness information from Kent (2005), the development of the chest stiffness scaling was possible. The intact thorax had a value of 1, the denuded thorax had a value of 0.87 and the eviscerated thorax had a value of 0.69.

The model of the thorax was assumed to be three springs in parallel. This assumption is made because it is observed that as additional elements are added to the eviscerated case, i.e. the flesh and viscera, the stiffness increases. Since the normalized total stiffness, k_T, is known to be 1 and the stiffness of the ribs, k_R, is known to be 0.69, the stiffness of the viscera, k_V, and flesh, k_F, are also known from the following relations:

$$k_F + k_V + k_R = k_T = 1$$

and,

$$k_V + k_R = 0.87$$

and,

$$k_R = 0.69$$

The relative contributions of the flesh, the viscera and the ribs are known to be:

$$k_F = 0.23$$
$$k_V = 0.18$$
$$k_R = 0.69$$

A stiffness ratio can be found between the child and the adult, represented as 1 and 2, respectively,

$$\frac{k_1}{k_2} = \frac{k_{T1}}{k_{T2}} = \frac{k_{F1} + k_{V1} + k_{R1}}{k_{F2} + k_{V2} + k_{R2}}$$

It was assumed that the stiffness of the flesh and the viscera is constant between the adult and the child and that the ribs themselves are geometrically similar their stiffness values can be scaled as done in Equation A2.

The stiffness ratio is then known to be

$$\lambda_K = \frac{k_1}{k_2} = \frac{k_{F1} + k_{V1} + \lambda_E \lambda_L k_{R2}}{k_{F2} + k_{V2} + k_{R2}}$$
$$= \frac{0.23 + 0.18 + 0.69\lambda_E \lambda_L}{0.23 + 0.18 + 0.69} = 0.31 + 0.69\lambda_E \lambda_L$$

Since the stiffness ratio is known the force scaling ratio is also known,

$$\lambda_F = \lambda_K \lambda_L = (0.31 + 0.69\lambda_E \lambda_L)\lambda_L$$

APPENDIX B: Video Analysis

In the case of the head CG, the knee and the H-point, approximations of the point of interest had to be inferred. In order to account for out-of-plane rotations of the head that resulted in perceived movement of the head CG target on a planar projection, the location of the head CG points was determined by the head outline at the following locations: the highest point, the most leftward, the most rightward, and the lowest point. This method for approximating the location of the head CG by tracking the location of the centroid of the projected head area is shown in Figure B1.

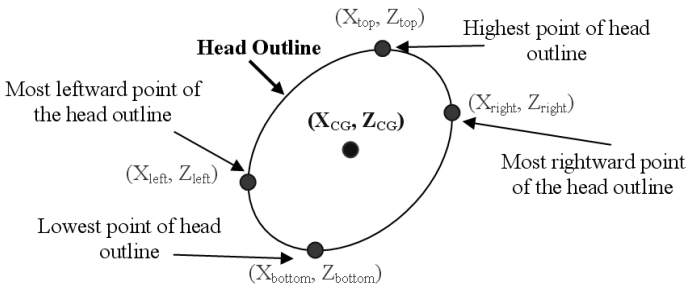

Figure B1: Approximation of the head CG of the pediatric cadaver by tracking the centroid of the head.

The head CG points could then be approximated as,

$$X_{CG} = \frac{X_{left} + X_{right}}{2}, Z_{CG} = \frac{Z_{top} + Z_{bottom}}{2} \quad [B1]$$

In order to find an approximate location for the knee joint, points were taken where leg meets the thigh above and below the actual location of the knee joint. The location of these points and their practical placement can be seen in Figure B2.

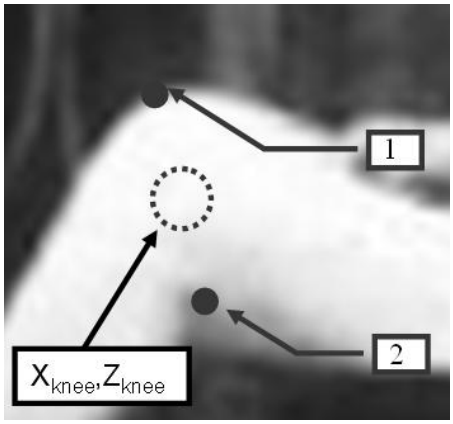

Figure B2: Determination of the location of the knee joint in the pediatric cadaver video analysis.

Once the location of these two points on the leg are determined, labeled 1 and 2 in Figure B2, the approximate location of the knee joint is,

$$X_{knee} = \frac{X_1 + X_2}{2}, Z_{knee} = \frac{Z_1 + Z_2}{2} \quad . \quad [B2]$$

Once the location of the knee joint is known then a method of finding the approximate location of the H-point, using the knee joint, can be utilized. This approach was taken because the location of the hip marker was observed to move during the test as the cadaver's clothing moved As shown in Figure B3, points are taken along the top of the thigh between the knee and hip.

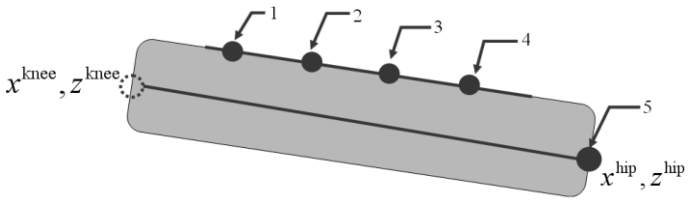

Figure B3: Method used for finding the approximate location of the H-point of the pediatric cadaver.

Using points 1, 2, 3, and 4, which are four points along the top of the thigh, a least squares slope was found through those points. It is assumed that this least squares slope is the same as the slope between the knee and the hip. Validation of this technique was performed by overlaying the approximate hip points on the video of the test. It was observed that the approximate hip points predicted the location of the hip more accurately than the photo target. The length of the femur was not listed in the cadaveric anthropometric data so its length was estimated (Snyde, 1977). By matching the known measurements of body weight, body length, and seated height with average measurements in the database, an age range based on the cadaver's anthropometry was determined based on those measurements rather than the subject age. With the assumed femur length and thigh angle, the approximate location of the H-point was determined based on the previously calculated knee joint location.

APPENDIX C: Comparison of HIII 5th Female to HIII 10-year old dummies

In the comparison of the belt forces and head CG accelerations between the HIII 10-year old and the scaled Hybrid III 5th female (Figure C1 a-e), the general trends as well as the approximate magnitudes of the data peaks are similar. Since data obtained from the HIII 10-year old and the scaled AF5 appeared to be an approximately equivalent, the scaling method will be used to scale between the dummies and the pediatric cadaver.

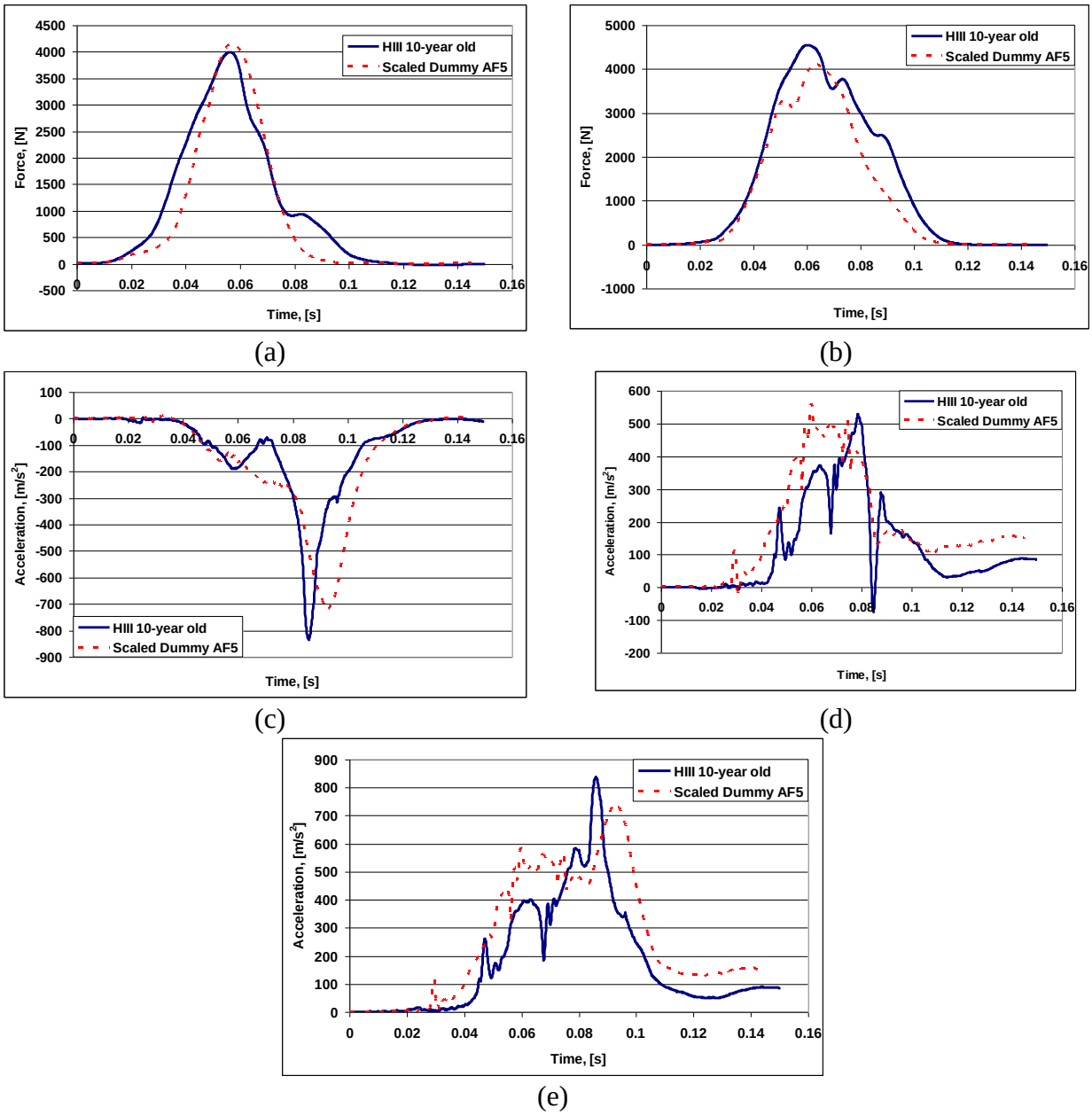

Figure C1 a,b) Scaled seat belt load of the lap and shoulder belts, respectively. c-e) Scaled accelerations for the X component, Z component, and resultant, respectively.

Kinematic Scaling

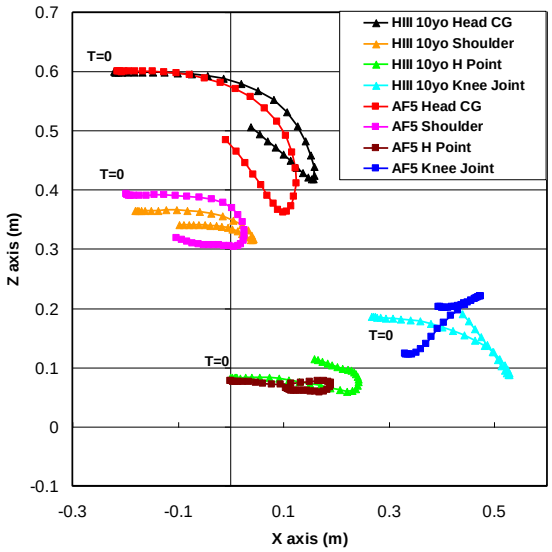

Figure C2: HIII 10-year old and AF5 kinematic trajectories

The kinematic trajectories scaled between the HIII 10-year old and the AF5 shown in Figure C3 show that the trajectories can be scaled between the dummies and that the excursion of the head, which is particularly important when analyzing child dummy kinematics, differed by less than 3 cm. All other points showed similar kinematics between the dummies with the exception of the knee joint. The reasons for the differences in the knee joint trajectories between the dummies were due to violations in geometric similarity, more specifically the violation of homologous points. These violations were seen in the seating positions of the two dummies (Figure C4). Since the foot of the Hybrid III 5th resides on the footrest of the buck, the knee joint was forced upward as the entire dummy translated forward. This motion was not seen in the HIII 10-year old where the knee would sink into the seat padding as the dummy was restrained by the belt system. The neck assembly of the HIII 10-year old dummy, seen in Figure C4, was in a more posterior position than the AF5 dummy. To correct this, the initial position of the HIII 10-year old was adjusted to begin at a similar X position as the AF5.

(a) (b)

Figure C4: HIII 10-year old (a) and AF5 dummy (b) seated position.

APPENDIX D: Scaled pediatric cadaver and AF5 graphed with HIII-10 year old acceleration and belt load

The shoulder belt loads and head CG accelerations of the pediatric cadaver and AF5 were scaled to the HIII 10-year old.

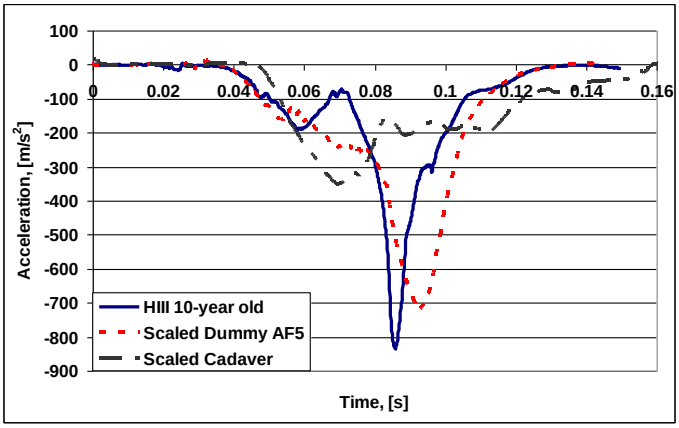

(a)

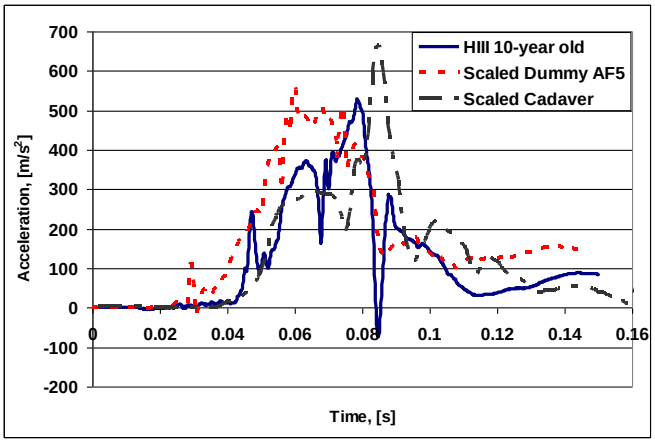

(b)

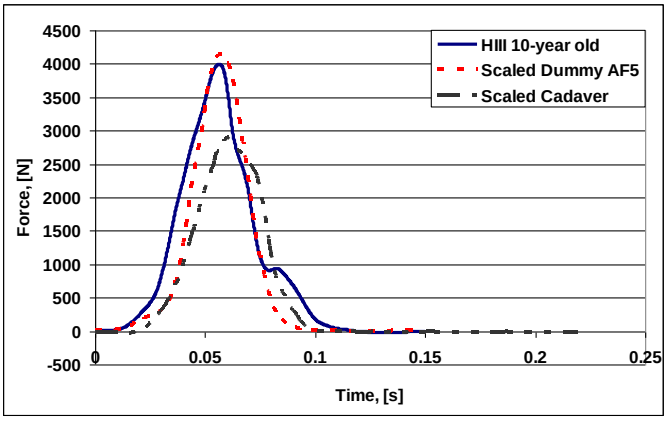

(c)

Figure D1: The scaled X and Z components of the head CG acceleration (a and b, respectively) are shown along with the shoulder belt load (c).

AUTHOR LIST

1. Joseph H. Ash
   1011 Linden Avenue
   Charlottesville, VA 22902
   434-296-7288 x138
   jash@virginia.edu

2. Christopher P. Sherwood
   1011 Linden Avenue
   Charlottesville, VA 22902
   434-296-7288
   CSherwood@iihs.org

3. Yasmina Abdelilah
   1011 Linden Avenue
   Charlottesville, VA 22902
   434-296-7288
   ya7w@virginia.edu

4. Jeff R. Crandall
   1011 Linden Avenue
   Charlottesville, VA 22902
   434-296-7288 x131
   jrc2h@virginia.edu

5. Daniel P. Parent
   1011 Linden Avenue
   Charlottesville, VA 22902
   434-296-7288 x127
   dpp6h@virginia.edu

6. Dimitrios Kallieris
   Vossstr. 2
   Heidelberg, Germanny
   Dimitrios_Kallieris@med.uni-heidelberg.de